Original Article

JOURNAL OF REINFORCED PLASTICS & COMPOSITES

Journal of Reinforced Plastics and Composites
0(0) 1–14

DOI: 10.1177/0731684415571191
jrp.sagepub.com

SAGE

Finite element modeling of fiber reinforced polymer bars embedded in prismatic concrete beams under high temperatures

Ali Zaidi[1], Kaddour Mouattah[1], Radhouane Masmoudi[2] and Brahim Hamdi[1]

Abstract

Numerous experimental tests and analytical investigation were carried out on thermal effects on fiber reinforced polymer bars reinforced concrete structures. Nevertheless, the finite element modeling of thermal behavior of fiber reinforced polymer bars embedded in concrete was insufficiently analyzed, particularly, for asymmetric problems. This paper presents a nonlinear numerical study using ADINA finite element software to investigate the effect of the ratio of concrete cover thickness to fiber reinforced polymer bar diameter (c/d_b) on the distribution of transverse thermal stresses and deformations in fiber reinforced polymer bars and concrete cover for an asymmetric problem using prismatic concrete beams reinforced with fiber reinforced polymer bars submitted to high temperatures up to + 60°C. Also, to predict the thermal loads (ΔT_{cr}) that produce the first radial cracks within concrete and the thermal loads (ΔT_{sp}) which cause the splitting failure of the concrete cover as a function of the ratio of concrete cover thickness to fiber reinforced polymer bar diameter for an asymmetric problem. Nonlinear numerical results in terms of cracking thermal loads, thermal deformations, and thermal stresses are compared to those evaluated from analytical models and experimental tests.

Keywords

Asymmetric problem, fiber reinforced polymer, concrete, temperature, cracks, numerical simulation

Introduction

In the last decade, the use of fiber reinforced polymer (FRP) in concrete structures has increased because of their high tensile strength, high stiffness to weight ratio, light weight, and their resistance to corrosion and fatigue. However, the thermal incompatibility between FRP bar and concrete particularly in transverse direction consists a big problem in reinforced concrete structures. This thermal incompatibility induces tensile stresses, within concrete under temperature increase, that may cause splitting cracks and, eventually, deterioration of the bond between FRP bars and concrete. Extensive experimental and analytical researches were carried out to analyze the thermal effect on FRP bars embedded in concrete.[1–7,11–13] An experimental and analytical study was published recently by Bellakehal et al. on the behavior of concrete slabs reinforced with FRP bars subjected, simultaneously, to temperatures (−30 to 60°C) and mechanical loads. The results obtained from this study prove that ratios of concrete cover thickness to FRP bar diameter (c/d_b) varied from 1.3 to 2.8 are sufficient to avoid failure of concrete cover of glass FRP (GFRP) bars reinforced concrete slabs.[8] Some numerical works were carried out by Zaidi et al.[9] on thermal behavior of concrete cover

[1]Structures Rehabilitation and Materials Laboratory (SREML), University of Laghouat, Laghouat, Algeria
[2]Civil Engineering Department, Sherbrooke University, Sherbrooke, Canada

Corresponding author:
Ali Zaidi, University of Laghouat, B.P 37G Laghouat, 03000 Algeria.
Email: ali.zaidi@Usherbrooke.ca

surrounding FRP bars using concrete cylinders axially reinforced with GFRP bars submitted to temperature variations up to 60°C. Authors recommended a ratio c/d_b greater than or equal to 2 for FRP reinforced concrete elements under thermal loadings up to 60°C when the confining action of concrete is symmetric.[9,10] Nevertheless, many parameters need more investigation such as concrete cover thickness, FRP bar diameter, spacing between FRP bars, the shape of concrete elements, and temperature variations. In this paper, a nonlinear finite element model is developed to analyze the distribution of thermal stresses and deformations in concrete cover surrounding FRP bars for prismatic concrete beams subjected to temperature increase up to 60°C using ADINA program. This nonlinear analysis permits also to predict the thermal loads (ΔT_{cr}) producing the first radial cracks within concrete and the thermal loads (ΔT_{sp}) producing the splitting failure of concrete cover as a function of the ratio of concrete cover thickness to FRP bar diameter (c/d_b) for an asymmetric problem. A comparison between numerical, analytical, and experimental results in terms of cracking thermal loads, thermal deformations, and thermal stresses is presented.

Nonlinear finite element analysis

Finite element model

A nonlinear numerical model has been performed using ADINA software to investigate thermal stresses and deformations in prismatic concrete beams reinforced with GFRP bars subjected to temperature increase (ΔT) up to 60°C when the confining action of concrete is asymmetric, as shown in Figure 1 and Table 1. Because of the constant of axial deformations, the prismatic concrete beam was modeled by means of two-dimensional plane stress elements. As the symmetric of the cross-section of concrete beam respect to z–z axis, the study was carried out only for the half of the cross-section of GFRP reinforced concrete beams, as shown in Figure 1(b). The geometry of model was defined with polar coordinate system. Triangular elements with six nodes were used for the meshing of the both concrete and GFRP bar (Figure 2). The temperature variation (ΔT) applied statically on the concrete and GFRP bar was increased with an increment of +5°C as shown in Figure 3. A perfect bond was considered between concrete and FRP bar. Both the materials (rebar and concrete) share the same nodes at the interface of FRP bar/concrete. The concrete used in this study was considered to have a nonlinear behavior. For the failure criterion, the maximum stress failure criterion was used by ADINA which consists to compare each component of stress tensor (referred to the material principal directions) to maximum stresses values of concrete. In this investigation, splitting cracks occur when the maximum tensile stress in the circumferential direction reaches the tensile strength of concrete. For the crack propagation, ADINA uses "the node shift/release" technique which consists to combine the shifting and the releasing of the successive crack tip nodes in order to model the propagation of the crack tip through the finite element mesh. The mechanical and physical properties of the concrete are presented in Table 2. The average tensile strength (f_{ct}) of concrete was determined by splitting tests and the average compressive strength (f'_c) was evaluated by standard compression tests.[14,15] The modulus of elasticity of concrete (E_c) was evaluated according to CAN/CSA-S806-02 guidelines,[4] while

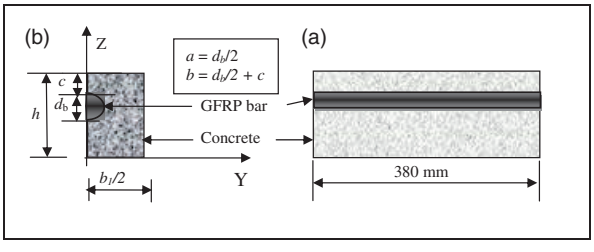

Figure 1. GFRP bar reinforced concrete beam modeled: (a) Rectangular prismatic concrete beam reinforced with GFRP bar, (b) half of the cross-section.

Table 1. Detail of rectangular prismatic concrete beams reinforced with GFRP bars.

Specimens	Spec. width b_1 (mm)	Spec. height h (mm)	Bar diameter d_b (mm)	Concrete cover thickness c (mm)	c/d_b
P.10.20[a]	76	100	9.5	20	2.1
P.13.20	76	100	12.7	20	1.6
P.13.25	76	100	12.7	25	2.0
P.13.30	76	100	12.7	30	2.5
P.16.20	76	100	15.9	20	1.3
P.16.25	76	100	15.9	25	1.6
P.16.30	76	100	15.9	30	1.9
P.19.20	100	125	19.1	20	1.0
P.19.25	100	125	19.1	25	1.3
P.19.30	100	125	19.1	30	1.6
P.25.25	100	150	25.4	25	1.0
P.25.30	100	150	25.4	30	1.2
P.25.35	100	150	25.4	35	1.4

[a]P: Prismatic concrete beam; 10: nominal diameter GFRP bar; 20: concrete cover thickness in mm.

the Poisson's ratio of concrete (ν_c) was assumed 0.17. The coefficient of thermal expansion (CTE) of concrete evaluated experimentally was found to be equal to $11.6 \pm 2.1 \times 10^{-6}/^{\circ}$C. Five GFRP bar diameters have been used in this study: 9.5, 12.7, 15.9, 19.1, and 25.4 mm. The sand-coated bars are made with E-glass fibers and vinyl ester resin and are manufactured by Pultrall. The transition temperature of the GFRP bars was determined by experimental tests and was found to be equal to $138 \pm 6^{\circ}$C. GFRP bars used had

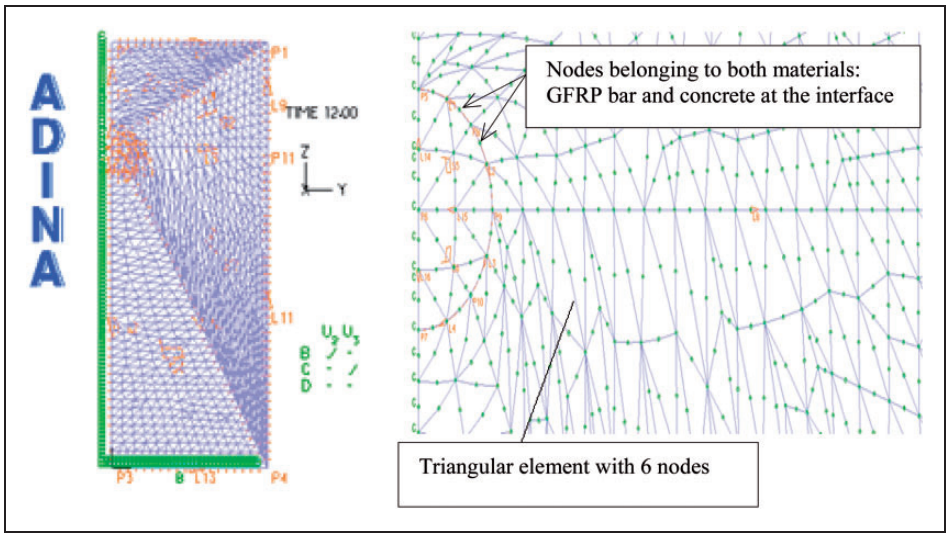

Figure 2. Meshing of the both concrete and GFRP bar.

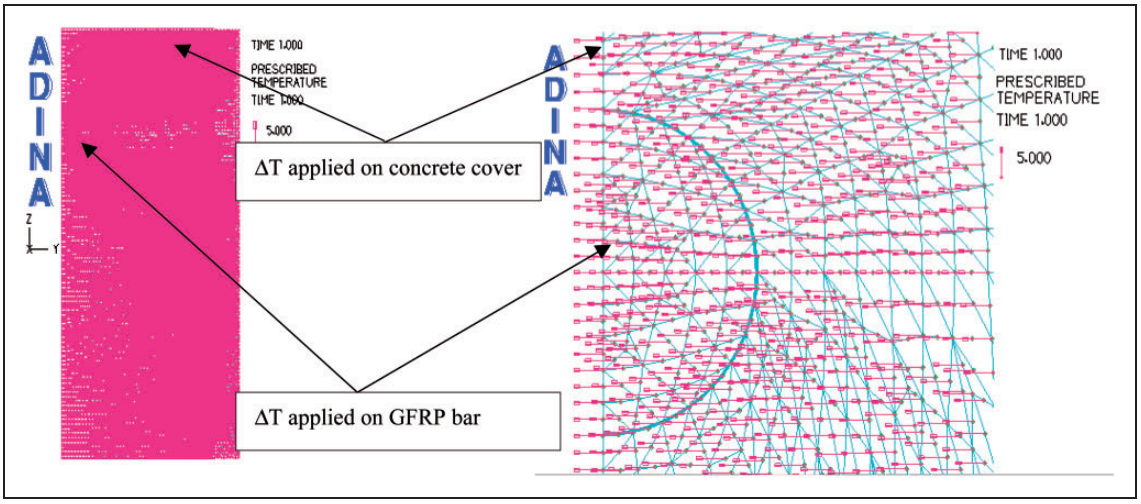

Figure 3. Temperature increase (ΔT) applied on the surface of both the GFRP bar and concrete of reinforced rectangular concrete beam specimen.

Table 2. Mechanical and physical properties of concrete.

Compressive strength f'_{c28}, MPa	Tensile strength f_{ct28}, MPa	Modulus of elasticity E_c, GPa	Poisson's ratio ν_c	Coefficient of thermal expansion α_c ($\times 10^{-6}/^{\circ}$C)
40 ± 3	4.1 ± 0.1	28 ± 2	0.17	11.6 ± 2.1

Table 3. Mechanical properties of the GFRP bars.

Bar diameter d_b, mm	Ultimate tensile strength f_{fu}, MPa	Longitudinal modulus of elasticity E_l, GPa	Longitudinal Poisson's ratio ν_{lt}
9.5	627 ± 22	42 ± 1	0.28 ± 0.02
12.7	617 ± 16	42 ± 1	0.28 ± 0.02
15.9	535 ± 9	42 ± 1	0.28 ± 0.02
19.1	600 ± 15	40 ± 1	0.28 ± 0.02
25.4	N/a	N/a	0.28 ± 0.02

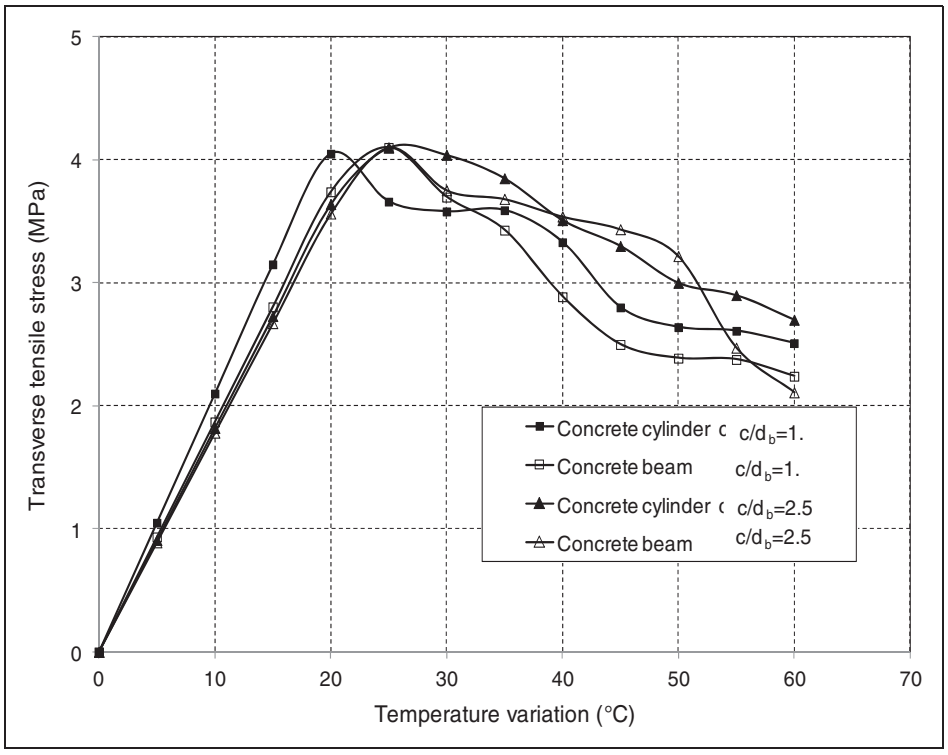

Figure 4. Numerical transverse tensile concrete stress at the interface—comparison between circular concrete cylinder and rectangular concrete beam for $c/d_b = 1$ and 2.5.

a linear elastic behavior. The mechanical properties of GFRP bars evaluated by experimental tests[2] are reported in Table 3. The modulus of elasticity (E_t) and Poisson's ratio (ν_{tt}) of GFRP bars in the transverse direction were determined theoretically using the rule of mixture and were found to be equal to 7.1 GPa and 0.38, respectively.[16] The average values of the transverse and the longitudinal CTE of GFRP bars for the five FRP bar diameters tested were found to be equal to $\alpha_t = 33 \pm 4 \times 10^{-6}$ and $\alpha_l = 8 \pm 1 \times 10^{-6}/°C$, respectively.[2] It should be noted that the mechanical and physical properties of GFRP bars and concrete used in this study were determined by Zaidi and Masmoudi.[2,7]

Numerical results and discussion

Figure 4 shows typical comparison of circumferential tensile stresses of concrete versus temperature variation at FRP bar/concrete interface for circular concrete cylinders studied by Zaidi and Masmoudi[9,10] and rectangular concrete beams reinforced with GFRP bars having ratios of concrete cover thickness to FRP bar diameter (c/d_b) equal to 1 and 2.5. From this figure, it can be seen that the thermal curves of the circumferential stress of concrete are almost linear up to 20 and 25°C from which the thermal curves decrease suddenly because the circumferential tensile stress in concrete reaches the tensile strength of concrete f_{ct} which is

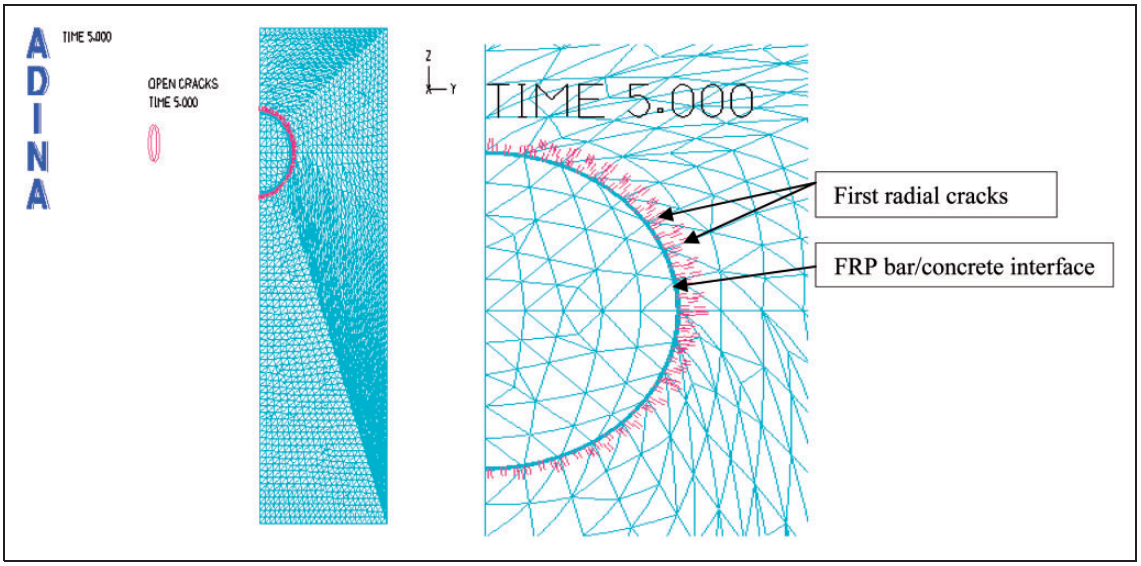

Figure 5. Appearance of the first radial cracks within concrete at FRP bar/concrete interface at thermal load ΔT_{cr} (for concrete beams having $c/d_b = 1.0$, $\Delta T_{cr} = 25°C$).

equal to 4.1 MPa. Also, it is observed that the first radial cracks start to develop in concrete at the interface at thermal loads (ΔT_{cr}) of 20 and 25°C for concrete cylinders and concrete beams, respectively, having ratios of $c/d_b \leq 1$. However, for ratios $c/d_b > 1$ the first radial cracks appear in concrete at 25°C for both the concrete cylinders and concrete beams. Figure 5 shows the appearance of the first radial cracks within concrete at FRP bar/concrete interface, obtained from ADINA software, at a temperature increase (ΔT_{cr}) of 25°C for concrete beams having a ratio c/d_b equal to 1.0. Table 4 presents the thermal load (ΔT_{sp}) producing the splitting failure of the concrete cover as versus the ratio of concrete cover thickness to FRP bar diameter (c/d_b) for GFRP reinforced concrete beams. At this thermal load (ΔT_{sp}), the radial cracks cannot be stopped and the concrete cover is completely cracked as shown in Figure 6. It can be observed that the thermal load ΔT_{sp} is varied from 50 to 60°C for a ratio c/d_b varied from 1.0 to 1.3. No cracks have been observed on the external surface of concrete beams subjected to thermal loadings (ΔT) up to 60°C and having a ratio of c/d_b greater than or equal to 1.4.

Figure 7 shows transverse thermal strains versus temperature variations (ΔT) at FRP bar/concrete interface of prismatic concrete beams reinforced with GFRP bars and having a ratio of concrete cover thickness to FRP bar diameter (c/d_b) varied from 1 to 2.5. It can be observed that the transverse thermal strains are linear and similar until ΔT equals to 30, 35, and 45°C corresponding to ratios of c/d_b ranged from 1 to 1.2, 1.3 to 1.9, and 2 to 2.5, respectively. From these thermal loads, the thermal strains increase suddenly because

Table 4. Nonlinear numerical thermal loads of splitting failure of concrete cover for GFRP bar reinforced rectangular prismatic concrete beams.

c/d_b	Splitting failure thermal load, ΔT_{sp} (°C)
1.0	50
1.2	55
1.3	60
≥1.4	>60

of the producing of the circular crown of splitting cracks, around FRP bars, which are great and profound. Also, it can be seen that for $c/d_b < 1.6$ the transverse thermal strains are important when $\Delta T \geq 30°C$ and can be reached 6000 $\mu\epsilon$ in average which is three times greater than that of specimens having $c/d_b \geq 1.6$. Figure 8 illustrates the effect of FRP bar diameter on the transverse thermal strain at the interface of FRP bar/concrete of an asymmetric problem with a constant concrete cover thickness equal to 20 mm varying FRP bar diameter. It can be seen that the FRP bar diameter has no big effect on the transverse thermal for $\Delta T \leq 30°C$. While for $\Delta T > 30°C$, the transverse thermal strain increases with the increase in the FRP bar diameter, as shown in Figure 8. The same observation can be noted for transverse thermal strains at the FRP bar/concrete interface of prismatic concrete beams reinforced with constant FRP bar diameter varying

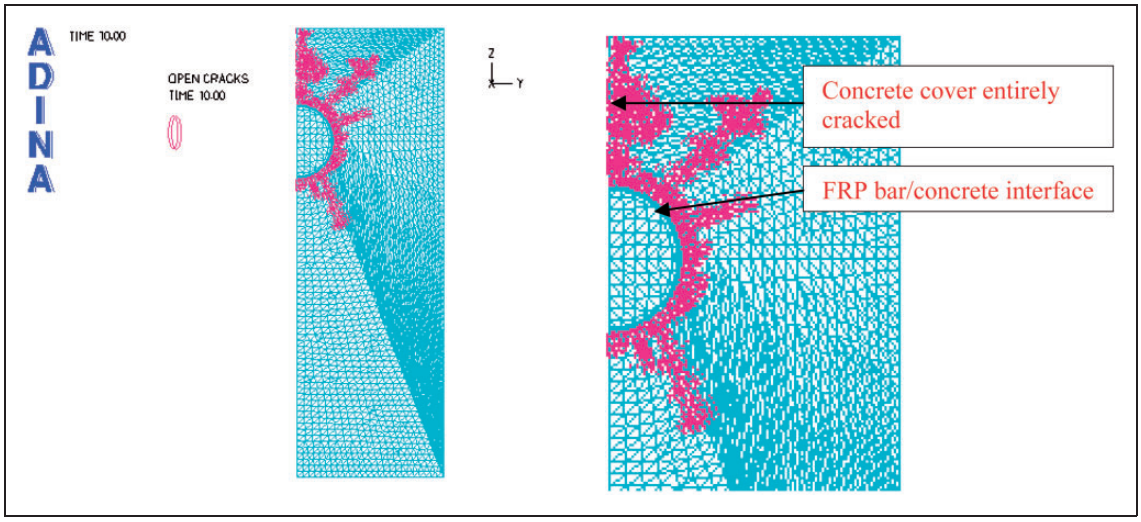

Figure 6. Failure of concrete cover ($\Delta T_{sp} = 50^{\circ}$C, beam P.25.25, $c/d_b = 1.0$).

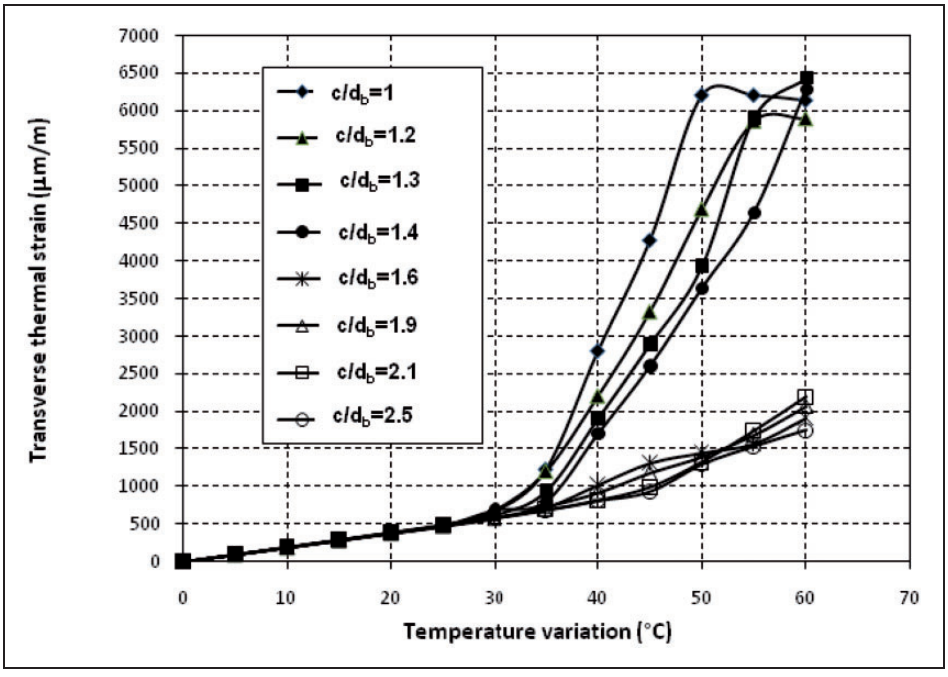

Figure 7. Numerical transverse thermal strains at FRP bar/concrete interface for reinforced prismatic concrete beams having different ratios of c/d_b.

concrete cover thickness (20, 25, 30 mm), as shown in Figure 9.

Figures 10 and 11 present the transverse thermal strains curves at the external surface of concrete cover of rectangular prismatic concrete beams reinforced with GFRP bar having a ratio c/d_b varied from 1 to 2.5. From Figure 11, it is observed that for a ratio $c/d_b \leq 1.6$ transverse thermal strains curves are linear and similar until temperature increase of 45 and 55°C corresponding to ratios $c/d_b = 1$ and 1.2–1.6, respectively, from which the concrete thermal strains raise abruptly because of splitting cracks which reach the external surface of concrete cover or too close (Figure 12(b) and (c)). Nevertheless, for $c/d_b > 1.6$, transverse thermal strain curves are linear and similar, as shown in Figure 10. It can be concluded that ratios of $c/d_b > 1.6$ have no big influence on transverse thermal strains at the external surface of concrete cover of prismatic concrete beams reinforced with GFRP bars and subjected to temperature increase up to $+60^{\circ}$C.

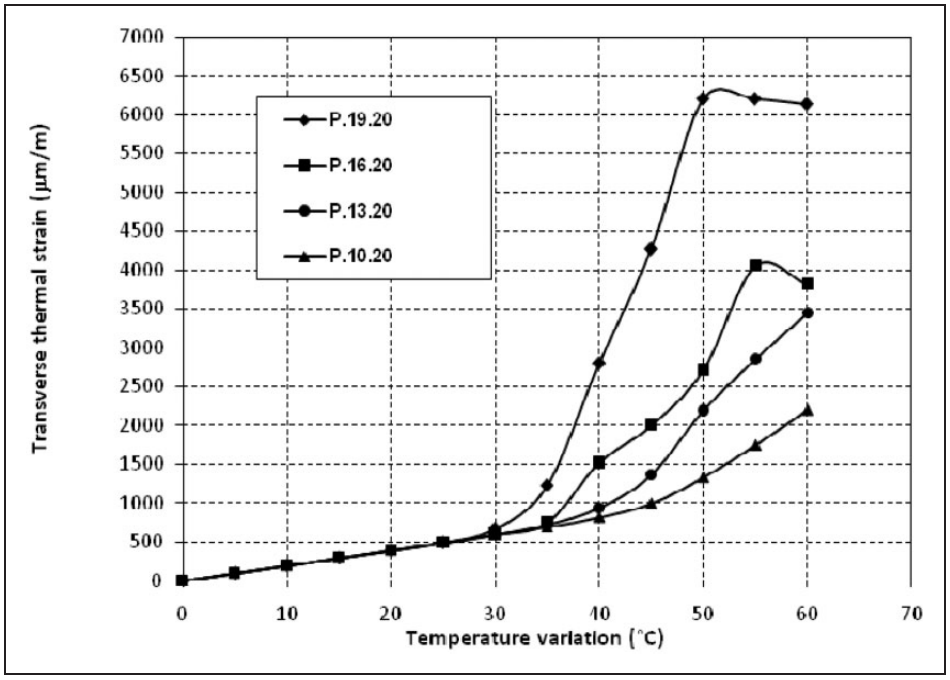

Figure 8. Numerical transverse thermal strains at FRP bar/concrete interface for prismatic concrete beams reinforced with different FRP bar diameters and having concrete cover thickness c = 20 mm. (P.19.20 = P: prismatic specimen; 19: nominal size of the bar (19.1 mm); 20 mm: concrete cover thickness.)

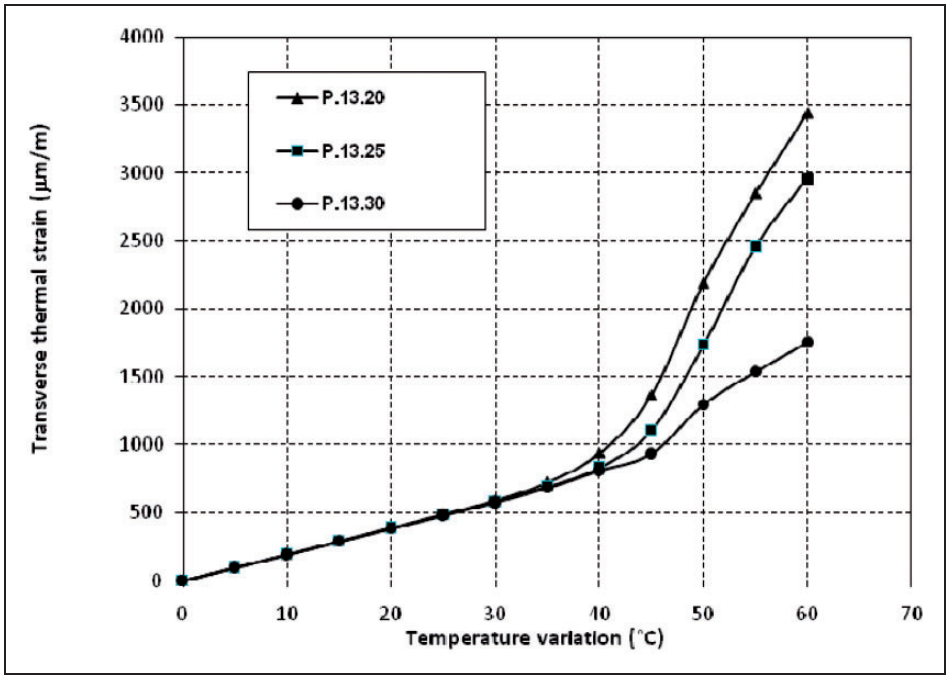

Figure 9. Numerical transverse thermal strains at FRP bar/concrete interface for prismatic concrete beams reinforced with 12.7 mm FRP bar diameter and having different concrete cover thickness. (P.13.20 = P: prismatic specimen; 13: nominal size of the bar (12.7 mm); 20 mm: concrete cover thickness.)

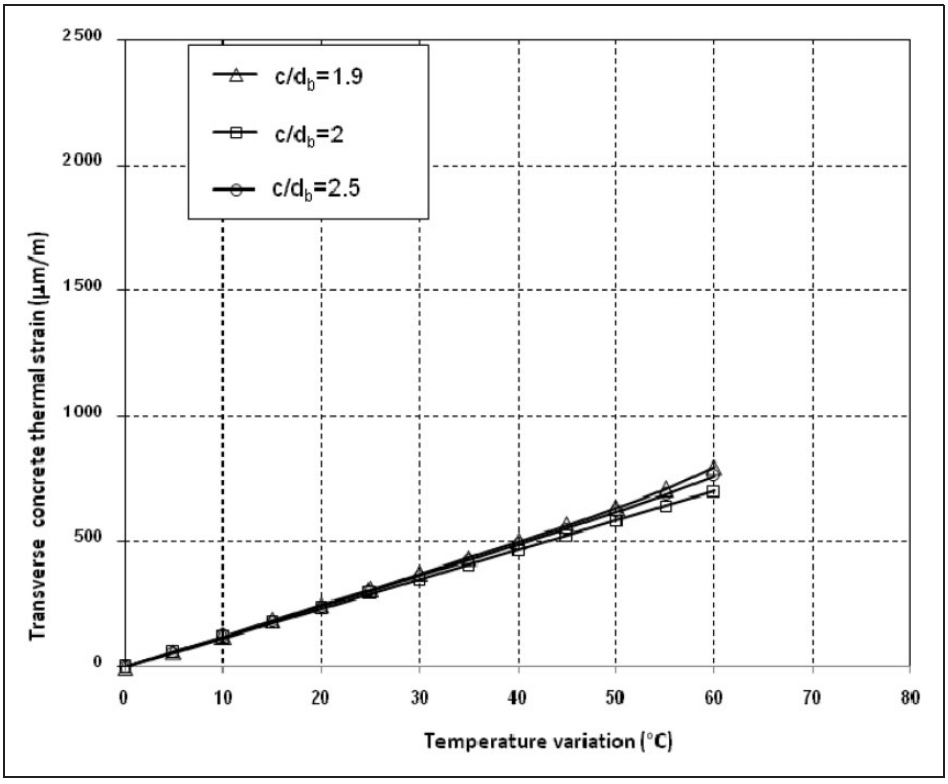

Figure 10. Numerical transverse thermal strains versus temperature variation at external surface of concrete cover for prismatic concrete beams having ratios $c/d_b > 1.6$.

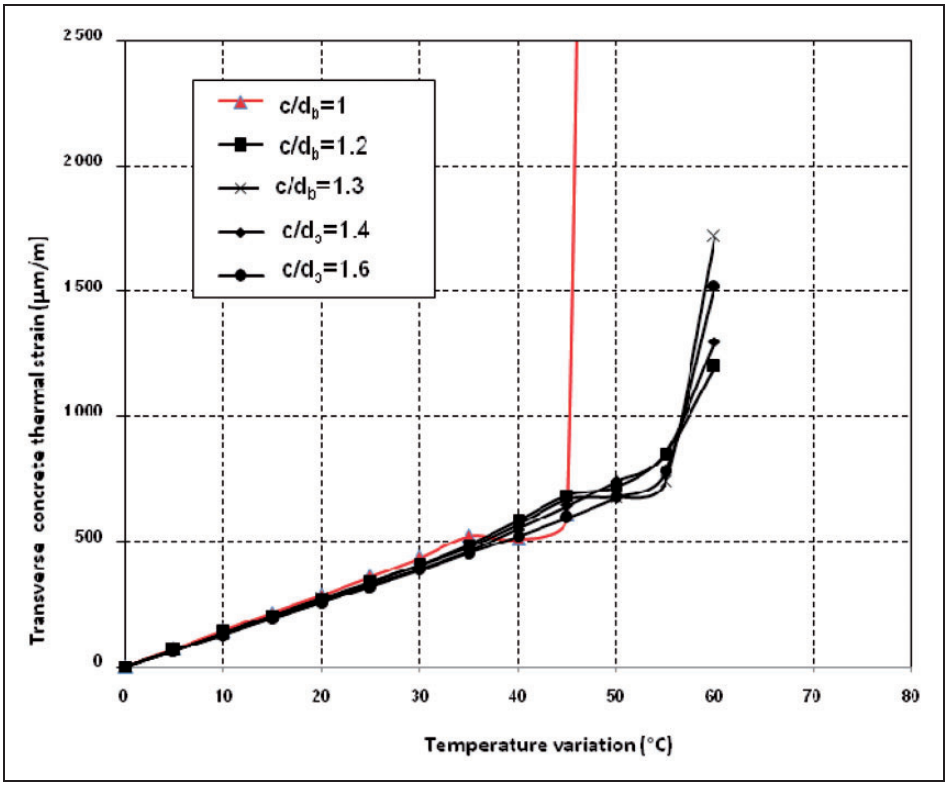

Figure 11. Numerical transverse thermal strains versus temperature variation at external surface of concrete cover for prismatic concrete beams having ratios $c/d_b \leq 1.6$.

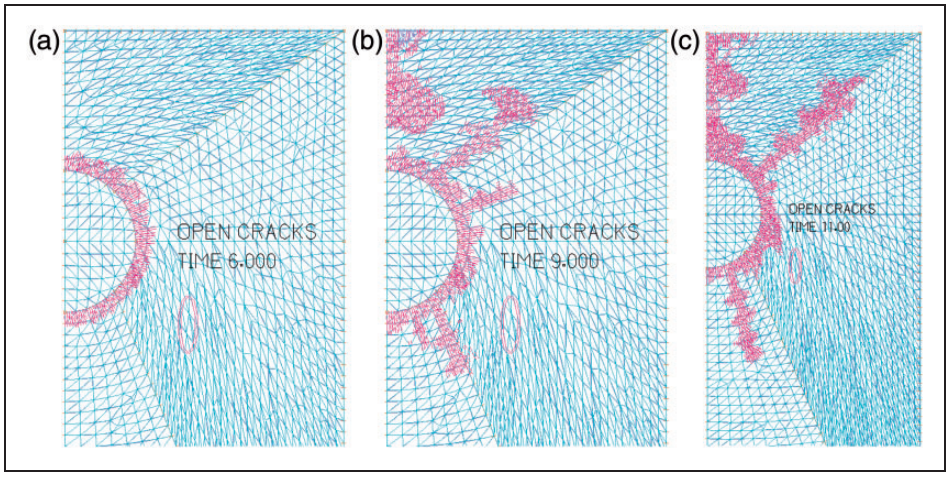

Figure 12. Radial cracks within concrete cover at FRP bar/concrete interface. (a) For $c/d_b = 1$, $\Delta T = +30^{\circ}C$; (b) for $c/d_b = 1$, $\Delta T = +45^{\circ}C$; (c) for $c/d_b = 1.2$, $\Delta T = +55^{\circ}C$.

Analytical background

The transverse thermal incompatibility between FRP bars and concrete generates radial pressure (P) at FRP bar/concrete interface under thermal loadings (ΔT). This radial pressure induces circumferential tensile stresses within concrete. From the analytical study carried out by Rahman et al.[5] and Masmoudi et al.,[3] the circumferential stress (σ_t) and the radial stress (σ_ρ) in a concrete element situated at a radius ρ from the center of the concrete cylinder reinforced with FRP bar due to radial pressure P are given by

$$\sigma_t = \frac{P}{r^2 - 1}\left(1 + \frac{b^2}{\rho^2}\right) \tag{1}$$

$$\sigma_\rho = \frac{P}{r^2 - 1}\left(1 - \frac{b^2}{\rho^2}\right) \tag{2}$$

where $r = b/a$ is the ratio of concrete cylinder radius ($b = c + d_b/2$) to FRP bar radius ($a = d_b/2$) ; P is the radial pressure at FRP bar/concrete interface which is given by

$$P = \frac{(\alpha_t - \alpha_c)\Delta T}{\frac{1}{E_c}\left(\frac{r^2+1}{r^2-1} + \nu_c\right) + \frac{1}{E_t}(1 - \nu_{tt})} \tag{3}$$

where E_c is the modulus of elasticity of concrete , ν_c is Poisson's ratio of concrete, α_c is the CTE of concrete, E_t is the modulus of elasticity of the FRP bar in the transverse direction, ν_{tt} is Poisson's ratio of the FRP bar in the transverse direction, and α_t is the transverse CTE of FRP bar.

Using equation (1) at the interface between concrete and FRP bar, at $\rho = a$, we obtain the maximum value of the circumferential tensile stress in concrete due to radial pressure P, given by

$$\sigma_{t\max} = \frac{r^2 + 1}{r^2 - 1} P = f_{ct} \tag{4}$$

The first radial crack appears in concrete at the FRP bar/concrete interface when the circumferential stress reaches the tensile strength of concrete f_{ct}.

Aiello et al.[6] proposed the following equation to predict the thermal load (ΔT_{sp}) that produces the splitting failure of the concrete cover for concrete cylinders reinforced with FRP bars (symmetric problems)

$$\Delta T_{sp} = \left[\frac{0.3 f_{ct}\, r}{E_c}[\ln(0.48r) + 1.6 + \nu_c] + \frac{0.3 f_{ct}\, r}{E_t}(1 - \nu_{tt})\right] \times \frac{1}{\alpha_t - \alpha_c} \tag{5}$$

Zaidi and Masmoudi[2] proposed the following relationship (equation (6)) to determine the thermal load (ΔT_{sp}) that produces the splitting failure of the concrete cover for rectangular prismatic concrete beams reinforced with GFRP bars (asymmetric problems)

$$\Delta T_{sp} = \frac{0.23 f_{ct}\, r}{(\alpha_t - \alpha_c)}\left[\frac{1}{E_c}[\ln(0.72\, r) + 3.2 + \nu_c] + \frac{1}{E_t}(1 - \nu_{tt})\right] \tag{6}$$

The transverse thermal strains in concrete (ε_{ct}) and in FRP bar (ε_{ft}), at the interface of FRP bar/concrete,

Table 5. Thermal loads of the splitting failure of concrete cover for beams and cylinders—comparison between numerical and analytical results.

	Aiello's equation	Zaidi's equation	Numerical model for cylinders[9,10]	Numerical model for beams
c/d_b	ΔT_{sp} (°C)	ΔT_{sp} (°C)	ΔT_{sp} (°C)	ΔT_{sp} (°C)
1.5	40	43.3	45	> 60
1.2	32.8	35.9	40	55
1	28.2	31.1	40	50

due to the radial pressure P and the temperature variation ΔT, are given by the following equations

$$\varepsilon_{ct}(a) = \frac{P}{E_c}\left(\frac{r^2+1}{r^2-1} + \nu_c\right) + \alpha_c \Delta T \tag{7}$$

$$\varepsilon_{ft}(a) = \alpha_t \Delta T - \frac{(1-\nu_{tt})}{E_t} P \tag{8}$$

However, the transverse thermal strain of concrete $\varepsilon_{ct}(b)$, at the external surface of concrete cover of rectangular prismatic concrete beams, due to the radial pressure P and the temperature variation ΔT, is given by

$$\varepsilon_{ct}(b) = \frac{2P}{E_c(r^2-1)} + \alpha_c \Delta T \tag{9}$$

Comparison between analytical, numerical, and experimental results

Cracking thermal loadings

Table 5 shows comparisons between thermal loads producing splitting failure of concrete cover obtained from analytical and numerical models for GFRP bars reinforced concrete beams and cylinders that have the tensile strength of concrete $f_{ct} = 4.1$ MPa. It can be observed that the thermal loads ΔT_{sp} predicted from numerical models for both concrete cylinders[9,10] and prismatic concrete beams are relatively greater than those obtained from analytical models (Zaidi's equation and Aiello's equation). This is probably due to the presence of healthy concrete elements which are not wholly cracked in the circular crown of the cracked concrete. These robust concrete elements resist well and delay the spalling of the concrete cover, however analytical models suppose that there is no tensile strength in the cracked concrete crown. Also, it is seen that numerical thermal loads ΔT_{sp} predicted for rectangular prismatic concrete beams are relatively higher with respect to those obtained for concrete cylinders.[9,10] Because the concrete cover thickness surrounding FRP bar is not constant in rectangular prismatic concrete beams (asymmetric problems), which reduces the tensile circumferential stresses through concrete cover. As a consequence, the splitting thermal loads ΔT_{sp} increase in rectangular prismatic beams. The same remarks can be noted for analytical splitting thermal loads predicted from Zaidi's equation, developed for rectangular prismatic concrete beams, compared to those obtained from Aiello's equation established for concrete cylinders.

Circumferential thermal stresses

Figures 13 and 14 present a typical comparison between analytical and numerical results in terms of circumferential tensile stresses of concrete versus temperature variations at FRP bar/concrete interface of concrete beams reinforced with GFRP bar having a ratio of concrete cover thickness to FRP bar diameter (c/d_b) equal to 1 and 2.5, respectively. These figures show that numerical and analytical curves of concrete beams are linear and similar for the temperature variation (ΔT) less than 25°C ($T < 45$°C since the reference temperature is 20°C); however, for the temperature variation greater than or equal to 25°C, the analytical curves become much greater because of the presence of radial cracks induced in concrete at the interface which is not considered in the analytical model based on the theory of elasticity.

Transverse thermal deformations

Figures 15 and 16 compare typical analytical and numerical transverse thermal strains, at the external surface of concrete cover, with those obtained from experimental tests carried out by Zaidi and Masmoudi[2] on rectangular prismatic concrete beams reinforced with GFRP bars under thermal loads up to +60°C, having ratios of c/d_b equal to 1.3 and 1.9, respectively. For a ratio $c/d_b = 1.3$ as shown in Figure 15, numerical and analytical results predicted from analytical and numerical models are in good agreement with experimental results until a temperature increase of 45°C from which

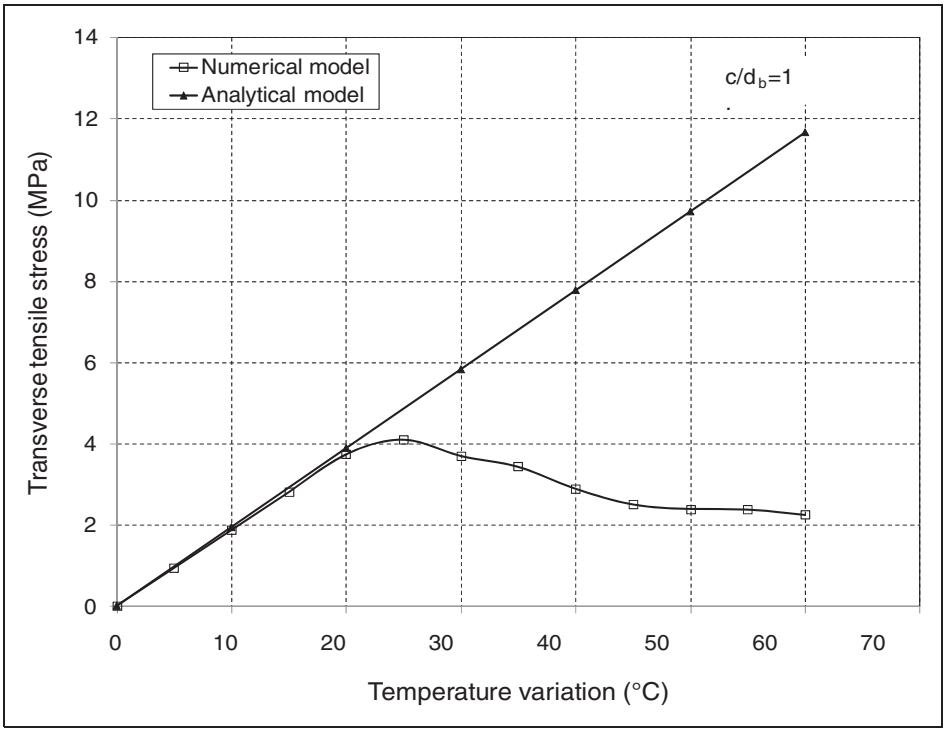

Figure 13. Transverse tensile concrete stress at FRP bar/concrete interface of concrete beam specimen P.25.25 having a ratio $c/d_b = 1$—comparison between numerical and analytical models.

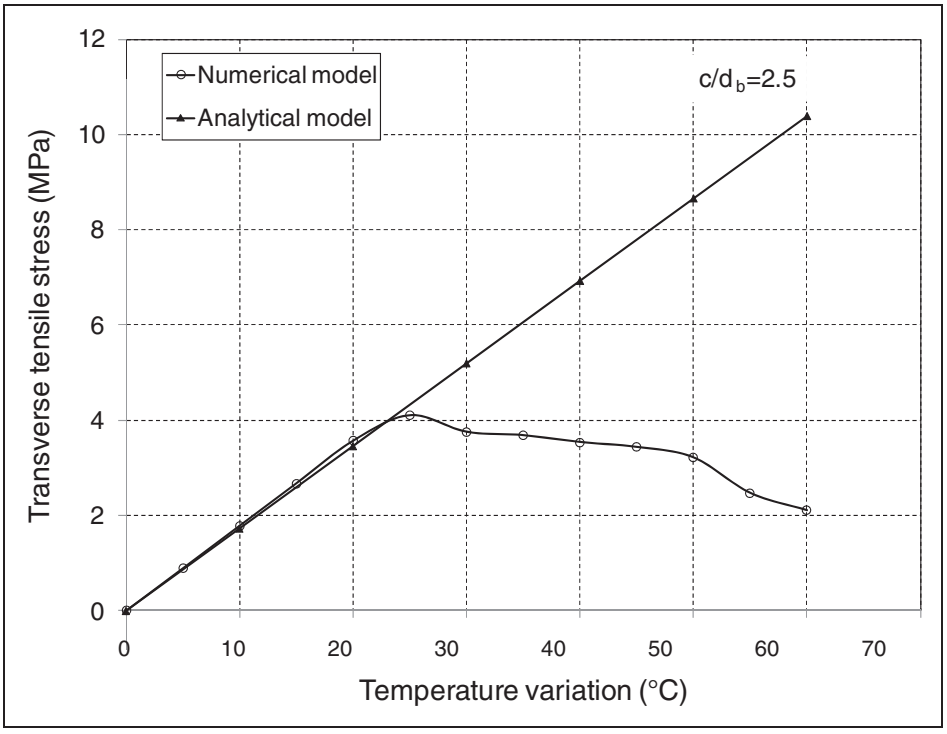

Figure 14. Transverse tensile concrete stress at FRP bar/concrete interface of concrete beam specimen P.13.30 having a ratio $c/d_b = 2.5$—comparison between numerical and analytical models.

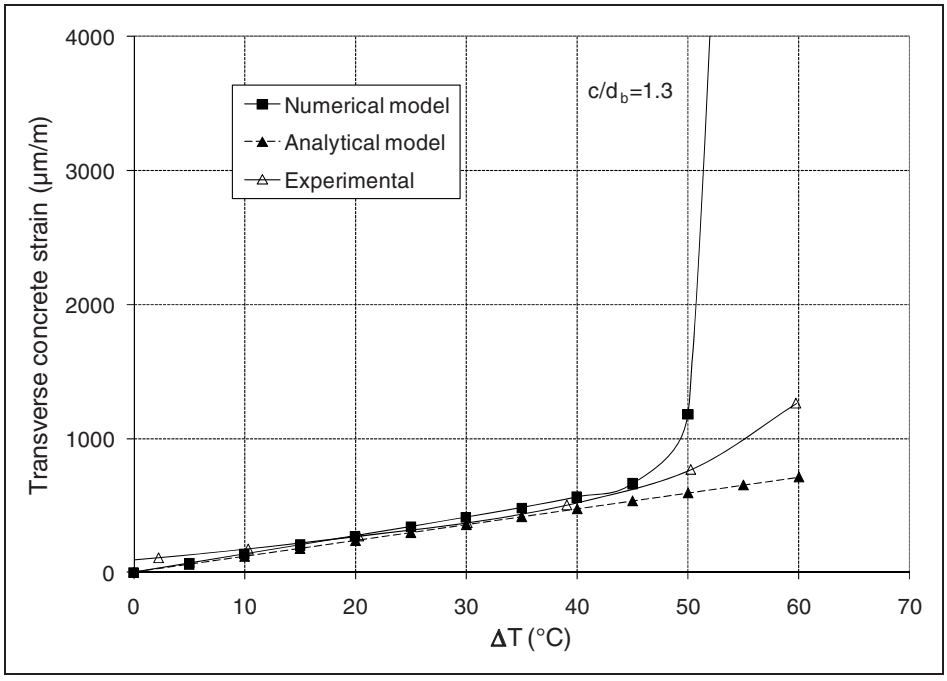

Figure 15. Transverse thermal strain at external surface of rectangular concrete beam specimen P.16.20 having a ratio $c/d_b = 1.3$—comparison between numerical, analytical, and experimental results.

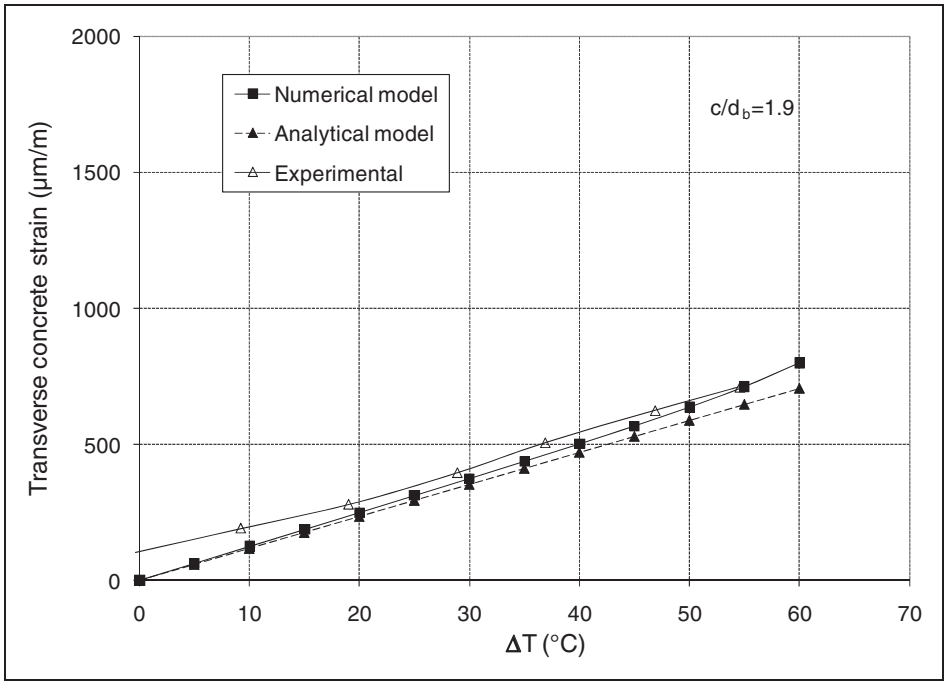

Figure 16. Transverse thermal strain at external surface of rectangular concrete beam specimen P.16.30 having a ratio $c/d_b = 1.9$—comparison between numerical, analytical, and experimental results.

numerical and experimental results are greater than those evaluated from analytical model because of profound splitting cracks, within concrete beams, which are not considered in the linear analytical model. While, for a ratio $c/d_b = 1.9$, numerical, analytical, and experimental strain curves are linear and similar, as shown in Figure 16, since there is no crack near the external surface of rectangular prismatic concrete beams.

Conclusions

1. First radial cracks appear in concrete at FRP bar/concrete interface at temperature increase ΔT_{cr} around $+25^{\circ}$C for rectangular concrete beams reinforced with GFRP bars having a ratio of concrete cover thickness to FRP bar diameter (c/d_b) varied from 1.0 to 2.5 and a concrete tensile strength of 4.1 MPa.
2. Thermal loads (ΔT_{sp}) obtained from the numerical model, producing the splitting failure of the concrete cover of rectangular concrete beams reinforced with GFRP bars under temperature variations (ΔT) up to 60°C, were found to be equal to 50, 55, and 60°C for ratios of c/d_b equal to 1, 1.2, and 1.3, respectively.
3. Thermal loads (ΔT_{sp}) predicted from numerical models for both concrete cylinders and rectangular prismatic concrete beams reinforced with GFRP bars are relatively greater than those obtained from analytical models. This is probably due to the presence of healthy concrete elements which are not wholly cracked in the circular crown of the cracked concrete.
4. Numerical thermal loads ΔT_{sp} predicted for rectangular prismatic concrete beams reinforced with GFRP bars are relatively higher with respect to those obtained for GFRP bars reinforced concrete cylinders. Because of the variable concrete cover thickness which reduces the tensile stresses in concrete surrounding FRP bars of prismatic concrete beams.
5. FRP bar diameter variation has no big influence on transverse thermal strains of rectangular prismatic concrete beams under a temperature increase $\Delta T \leq 30^{\circ}$C. However, for $\Delta T > 30^{\circ}$C the transverse thermal strain increases with the increase in FRP bar diameter. The same conclusion can be noted for the concrete cover thickness effect on transverse thermal strains.
6. The numerical transverse strain curves, at FRP bar/concrete interface of rectangular prismatic concrete beams under thermal loads up to $+60^{\circ}$C having c/d_b varied from 1 to 2.5, are linear and similar until thermal loads ΔT varied from $+30$ to $+45^{\circ}$C depending on c/d_b ratio. From these thermal loads, the transverse strain curves increase abruptly because of the circular crown of splitting cracks developed within concrete around FRP bars.
7. A ratio of concrete cover thickness to FRP bar diameter $c/d_b > 1.6$ with $\Delta T \leq 30^{\circ}$C seems to be sufficient to avoid harmful radial cracks within concrete surrounding GFRP bar under high temperatures for an asymmetric problem studied in this investigation.
8. For a ratio $c/d_b > 1.6$, the transverse thermal strains of concrete, at the external surface of concrete cover, predicted from numerical and analytical models are in good agreement with those obtained from experimental tests carried out on rectangular prismatic concrete beams reinforced GFRP bar submitted to thermal loads up to $+60^{\circ}$C.

Acknowledgements

The writers would like to acknowledge the support of the Department of Civil Engineering of Sherbrooke University (Canada) and also the Structures Rehabilitation and Materials Laboratory (SREML) of Laghouat University (Algeria). The opinion and analysis presented in this paper are those of the authors.

Conflict of interest

None declared.

Funding

This research received no specific grant from any funding agency in the public, commercial, or not-for-profit sectors.

References

1. Gentry TR and Husain M. Thermal compatibility of concrete and composite reinforcements. *J Compos Constr* 1999; 3: 82–86.
2. Zaidi A and Masmoudi R. Effect of concrete cover thickness and FRP-bars spacing on the transverse thermal expansion of FRP bars. In: *Eighth international symposium on fiber reinforced polymer reinforcement for concrete structures*. Patras, Greece: University of Patras, Department of Civil Engineering, 2007, pp.1–10.
3. Masmoudi R, Zaidi A and Gérard P. Transverse thermal expansion of FRP bars embedded in concrete. *J Compos Constr* 2005; 9: 377–387.
4. Canadian Standards Association. *Design and construction of building components with fiber-reinforced polymers. CAN/CSA–S806–02*, Toronto, Ontario, Canada, 2002.
5. Rahman HA, Kingsley CY and Taylor DA. Thermal stress in FRP reinforced concrete. In: *Proceedings of annual conference of the Canadian Society for Civil Engineering*. Ottawa, 1995, pp.605–614. Ottawa: CSCE.
6. Aiello MA, Focacci F and Nanni A. Effects of thermal loads on concrete cover of fiber reinforced polymer reinforced elements: theoretical and experimental analysis. *ACI Mater J* 2001; 98: 332–339.
7. Zaidi A and Masmoudi R. Effect of low and high temperatures on the transverse thermal expansion of FRP bars embedded in concrete. In: *Seventh international conference on short and medium span bridges*, Montreal, Quebec, Canada, August 2006, pp.1–11. Ottawa: CSCE.
8. Bellakehal H, Zaidi A, Masmoudi R, et al. Behavior of FRP bars-reinforced concrete slabs under temperature and sustained load effects. *Polymers* 2014; 6: 873–889.
9. Zaidi A, Masmoudi R and Bouhicha M. Numerical analysis of thermal stress-deformation in concrete surrounding FRP bars in hot region. *Constr Build Mater* 2013; 38: 204–213.

10. Zaidi A and Masmoudi R. Numerical analysis of the transverse thermal behaviour of FRP bars embedded in concrete. In: *Third international conference on durability and field applications of fiber reinforced polymer (FRP) composites for construction*. Quebec, Canada, May 2007, pp.1–8. Sherbrooke: Université de Sherbrooke.
11. Benmokrane B and El-Salakawy E. Durability and field applications of fibre reinforced polymer (FRP) composites for construction. In: *Proceedings of third international conference on durability and field applications of fibre reinforced polymer (FRP) composites for construction. CDCC-07*, Quebec City, Quebec, Canada, 2007, pp.1–569. Sherbrooke: Université de Sherbrooke.
12. Benmokrane B, El-Salakawy E and Ahmed E. Durability and sustainability of fibre reinforced polymer (FRP) composites for construction and rehabilitation. In: *Proceedings of fourth international conference on durability and sustainability of fibre reinforced polymer (FRP) composites for construction and rehabilitation. CDCC-11*, Quebec City, Quebec, Canada, 2011, pp.1–687. Sherbrooke: Université de Sherbrooke.
13. Zaidi A and Masmoudi R. Thermal effect on fiber reinforced polymer reinforced concrete slabs. *Can J Civ Eng* 2008; 35: 312–320.
14. American Society for Testing and Materials. Standard test method for splitting Tensile strength of cylindrical concrete specimens. *Annual book of ASTM standards ASTM C 496–96*, USA 2002; 04.2: 281–284.
15. American Society for Testing and Materials. Standard test method for compressive strength of cylindrical concrete specimens. *Annual book of ASTM standards ASTM C 39/C 39M–01*, USA 2002; 4.2: 21–25.
16. Gay D. *Matériaux composites*, 4th ed. Paris: Hermès, 1997.

Appendix 1

Notation

a	radius of FRP bar
b	radius of concrete cylinder
c	concrete cover thickness
d_b	bar diameter
E_c	modulus of elasticity of concrete
E_l	longitudinal modulus of elasticity of FRP bar
E_t	transverse modulus of elasticity of FRP bar
f'_c	compressive strength of concrete
f_{ct}	tensile strength of concrete
f_{fu}	ultimate tensile strength of FRP bar
P	radial pressure exerted by surrounding concrete on FRP bar
r	ratio of radius of cylinder to that of FRP bar $r = b/a$
α_c	coefficient of thermal expansion of concrete
α_t	transverse coefficient of thermal expansion of FRP bar
ΔT	temperature variation (thermal load)
ΔT_{cr}	thermal load producing the first radial cracks in concrete at FRP bar/concrete interface
ΔT_{sp}	thermal load producing the splitting failure of concrete cover
ε_{ct}	circumferential strains in concrete
ε_{ft}	circumferential strains in FRP bar
ν_c	Poisson's ratio of concrete
ν_{tt}	transverse Poisson's ratio of FRP bar
ν_{lt}	longitudinal Poisson's ratio of FRP bar
σ_ρ	radial stress
σ_t	circumferential stress